Supporting Information for

Visualizing nanoplastics-metal ions co-exposure stress with a NIR biothiols responsive fluorescent probe

Shaoyu Wei,[a,d] Liangwei Zhang,*[a,d] Jiangkun Tan,[a,d] Shudi Liu,[b] Maryam Arabi,[a] Abbas Ostovan,[a] Xuming Zhuang,[b] and Lingxin Chen*[a,c,d]

[a] Shandong Key Laboratory of Coastal Zone Environmental Processes and Ecological Security, Shandong Engineering Research Center for Coastal Zone Ecological & Environmental Monitoring Technologies and Equipment, Yantai Institute of Coastal Zone Research, Chinese Academy of Sciences, Yantai 264003, China. E-mail address: liangweizhang@yic.ac.cn (L. Zhang); lxchen@yic.ac.cn (L. Chen)

[b] College of Chemistry and Chemical Engineering, Yantai University, Yantai 264005, China

[c] Laboratory for Marine Biology and Biotechnology, Qingdao Marine Science and Technology Center, Qingdao 266237, China

[d] University of Chinese Academy of Sciences, Beijing 100049, China

Table of contents

1. General methods

Materials and instruments

All reagents were purchased from commercial suppliers without further purification. Silica gel P60 200-300 mesh was used from local reagent suppliers. All the tested solutions were prepared in ultrapure water via the Aquaplore water purification system (USA). The stock solution of probe 1 was prepared in DMSO and stored in the refrigerator at 4 °C and keeped dark.

Absorption spectra were measured from the Evolution220 UV-Visible spectrophotometer (Thermo). Fluorescence spectra were measured from fluorescence spectrophotometer (HITACHI F-4700). High resolution mass spectrometry (HRMS) was characterized on Waters HCLass XEVOG2XSQTof spectrometer. NMR spectra were recorded on Bruker AVANCE IIITM 500 spectrometer. The fluorescence imaging of cells were recorded on Olympus fluorescent microscope (Fluo View FV1000, Japan).

Cell culture

HeLa cells, Hep G2 cells, RAW 264.7 cells were purchased from the Cell Bank of Chinese Academy of Sciences (Shanghai, China). HeLa cells, Hep G2 cells, RAW 264.7 cells were cultured in high glucose DMEM (Dulbecco's modified eagle medium) (HyClone, USA) with 10% Fetal Bovine Serum (FBS) and 1% Penicillin-Streptomycin Liquid (Solarbio, China). The cells were plated on Petri-dishes according to the instructions from the manufacturer in a humidified atmosphere of 5% CO_2 and 95% air at 37 °C.

Laser confocal imaging

Confocal laser scanning microscopy was employed for cellular fluorescence imaging, using a ×40 objective for cells and a ×20 objective for zebrafish samples. Cells were cultured in dishes for 24 hours to allow adherence, followed by pretreatment according to the experimental protocol. Prior to fluorescence imaging, 1 mL of fresh complete culture medium was added to the dish for probe 1 incubation. The emission collection window was set to 580–650 nm, with excitation at 488 nm.

Cell cytotoxicity

The cytotoxicity of probe toward HepG2 cells was evaluated using the CCK-8 assay. A 100 µL aliquot of cell suspension and culture medium mixture at a density of 5×10^5 cells per well was seeded into each well of a 96-well plate and pre-incubated in an incubator at 37 °C with 5% CO_2 for 24 h. the probe was then added at concentration gradients of 0, 5, 10, 15, 20, 25, 30, 35, and 40 µM, with blank and control groups also set up. Three replicate wells were used for each concentration, and the cells were further cultured for 12 h. After incubation, the unbound probe and dead cells were washed away with PBS buffer. Subsequently, 100 µL of prepared complete medium containing 10% CCK-8 solution was added to each well, and the cells were incubated for an additional 4 h. Finally, the absorbance (OD value) at 450 nm was measured using a microplate reader, and the cell viability was calculated to assess the cytotoxicity of probe 1. Cell viability (%) = (OD value of experimental group − OD value of blank group) / (OD value of negative control group − OD value of blank group) × 100%.

2. Synthesis of the probe

Synthesis of compound 1 Compound 1 was synthesized according to the previous work.

Synthesis of compound 2 Compound 1 (297 mg, 1 mmol) and pyridinium (352 mg, 1.5 mmol) were dissolved in anhydrous ethanol. Subsequently, a catalytic amount of piperidine was added, and the mixture was heated to 80°C and refluxed for 5 h. After the reaction was completed, the mixture was cooled to precipitate a solid. The crude product was isolated by suction filtration. ^{1}H NMR (500 MHz, DMSO) δ 8.52 (d, *J* = 6.9 Hz, 2H), 8.48 (dd, *J* = 7.9, 1.3 Hz, 1H), 8.37 (s, 1H), 8.26 (dd, *J* = 7.4, 1.3 Hz, 1H), 8.11 (d, *J* = 15.6 Hz, 1H), 7.97 (d, *J* = 7.0 Hz, 2H), 7.89 (d, *J* = 15.6 Hz, 1H), 7.42 (t, *J* = 7.6 Hz, 1H), 4.11 (s, 3H), 4.03 – 4.00 (m, 2H), 1.57 (dt, *J* = 14.9, 7.5 Hz, 2H), 1.33 (dd, *J* = 14.9, 7.4 Hz, 2H), 0.92 (t, *J* = 7.4 Hz, 3H). ESI-MS: $[M+H]^+$, 387.28

Synthesis of probe Under an argon atmosphere, compound 2 (194 mg, 0.5 mmol) was dissolved in 10 mL of anhydrous dichloromethane. Triethylamine (101 mg, 1 mmol) was then added, and the mixture was stirred for 30 min. Subsequently, acryloyl chloride (0.16 mL, 2 mmol) was added, and the mixture was stirred at room temperature for 24 h. The reaction progress was monitored by TLC during the process. The crude product was purified by silica gel column chromatography. ^{1}H NMR (500 MHz, DMSO) δ 8.97 (t, 3H), 8.55 (d, *J* = 7.3 Hz, 1H), 8.40 (d, *J* = 6.8 Hz, 2H), 8.25 (d, *J* = 8.4 Hz, 1H), 8.05 (d, *J* = 16.4 Hz, 1H), 7.94 (dd, *J* = 21.9, 12.2 Hz, 2H), 6.77 (qd, *J* = 17.3, 5.7 Hz, 2H), 6.42 (dd, *J* = 9.8, 1.6 Hz, 1H), 4.31 (s, 3H), 4.08 (t, *J* = 7.3 Hz, 2H), 1.64 (dd, *J* = 14.7, 7.6 Hz, 2H), 1.38 (dd, *J* = 14.9, 7.4 Hz, 2H), 1.33 – 1.26 (m, 1H), 0.94 (t, *J* = 7.4 Hz, 3H). ^{13}C NMR (125 MHz, DMSO) δ 164.41, 163.48, 163.02, 151.75, 149.67, 145.91, 136.04, 132.12, 131.85, 129.95, 129.32, 129.02, 128.76, 127.09, 126.85, 125.89, 124.84, 123.22, 121.61, 47.61, 30.06, 20.20, 14.20, 0.55. ESI-MS: $[M+H]^+$, 441.29.

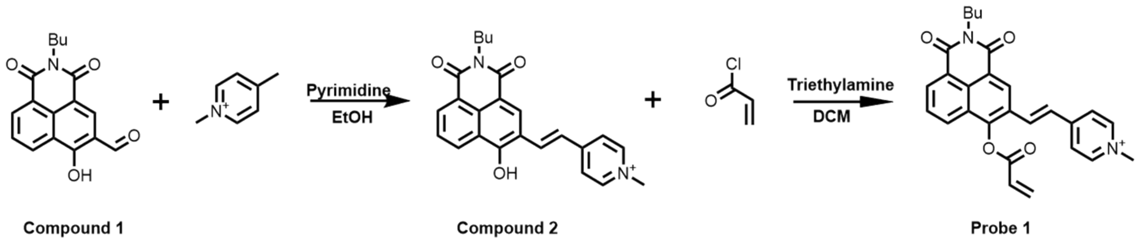

Scheme S1. Synthesis route of probe 1

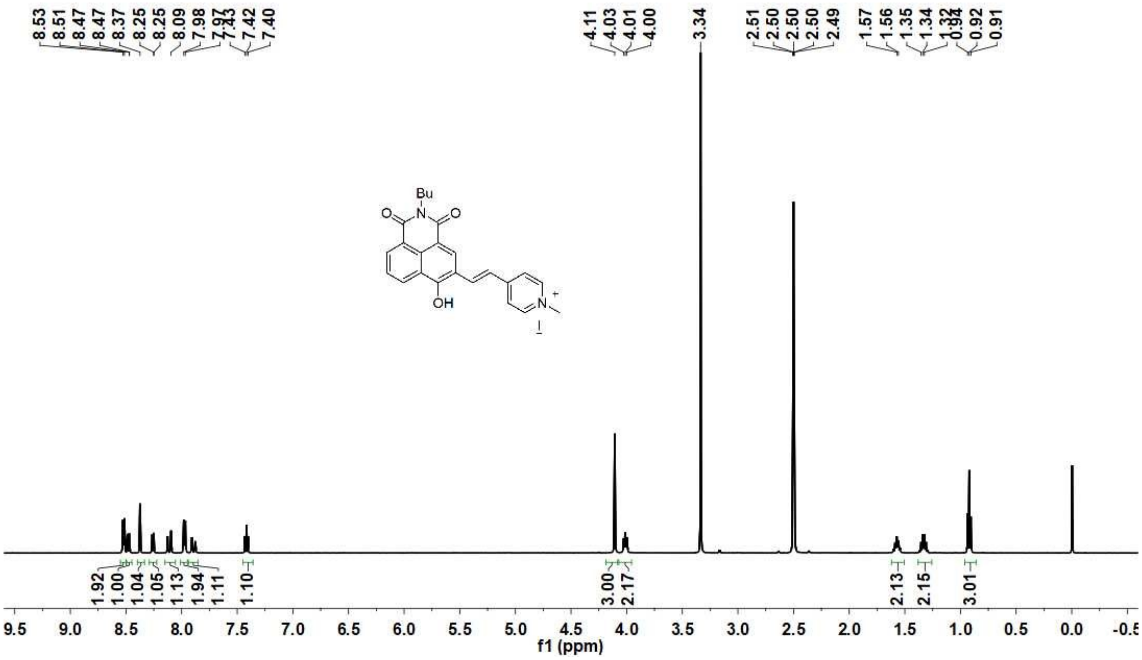

Fig. S1 ^{1}H NMR septrum of the compoud 2

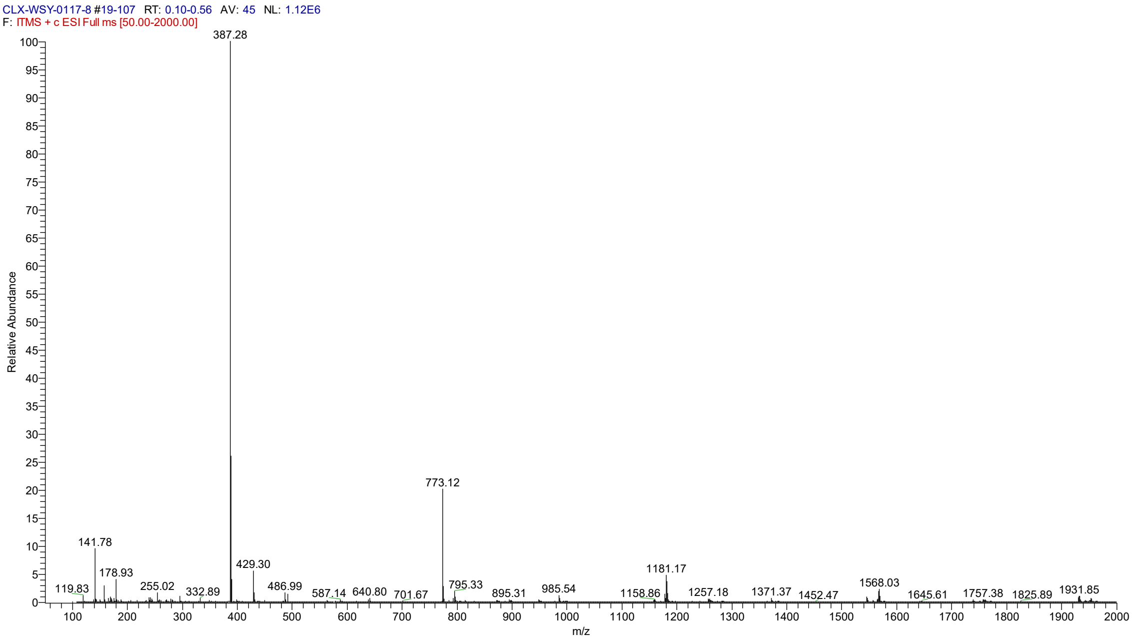

Fig. S2 The mass septrum of the compound 2

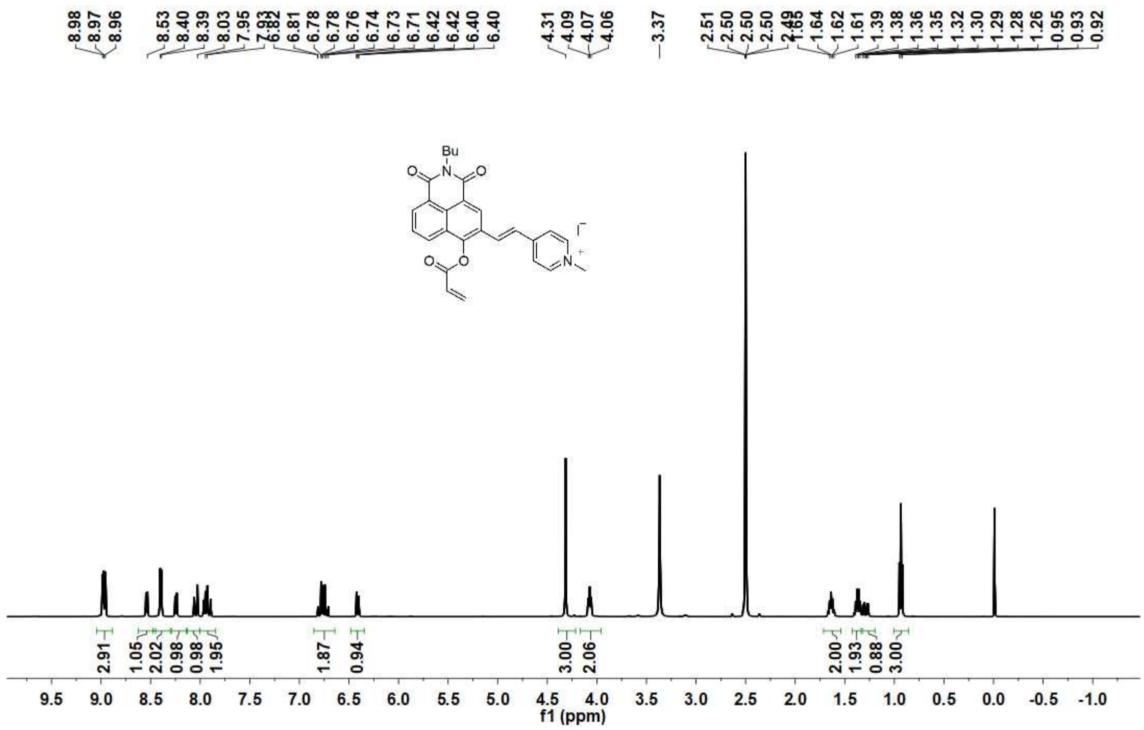

Fig. S3 ^{1}H NMR septrum of the probe

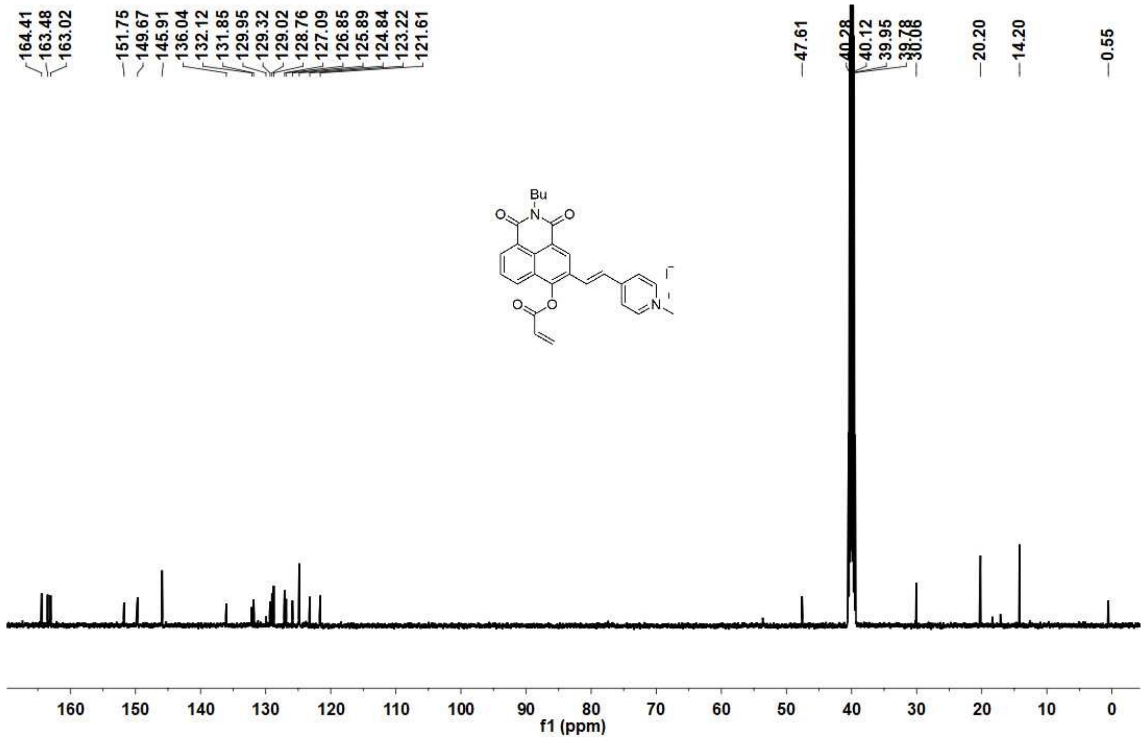

Fig. S4 ^{13}C NMR septrum of the probe

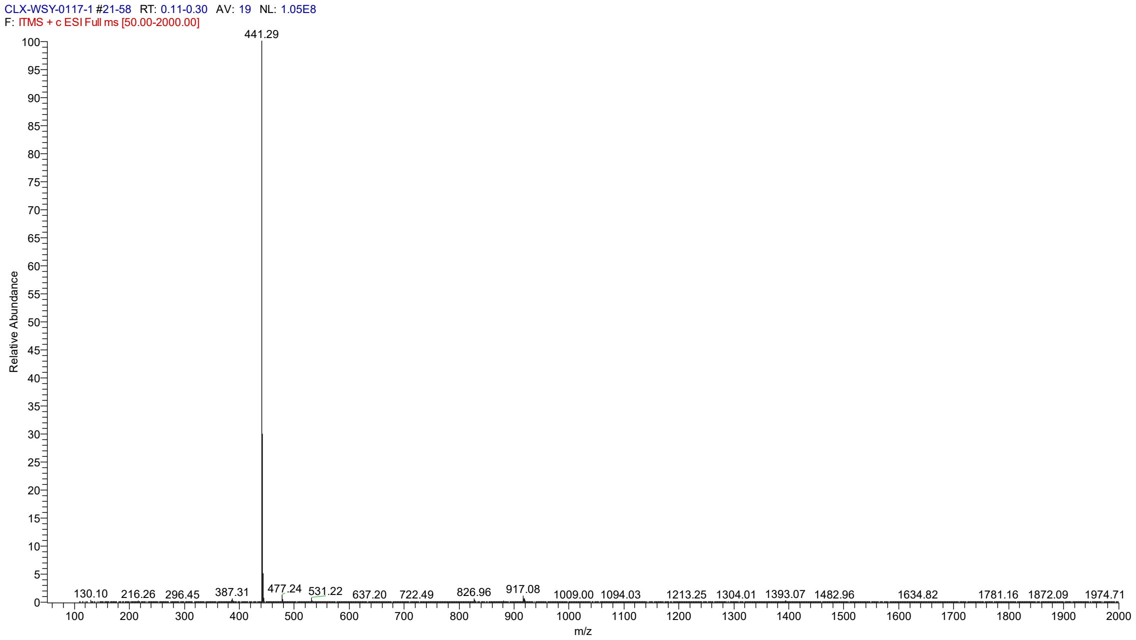

Fig. S5 The mass septrum of the probe

3. Molar extinction coefficient of the probe

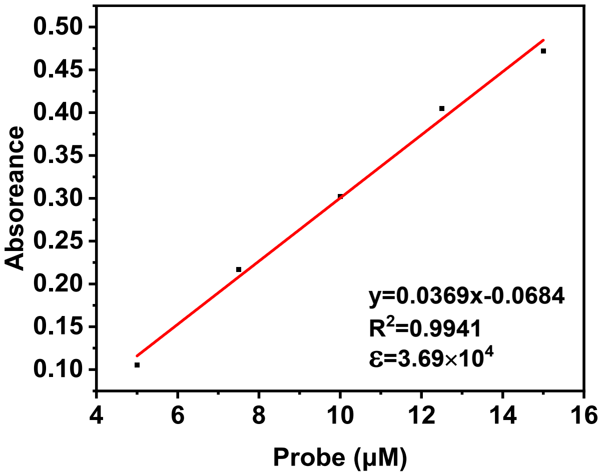

Fig. S6 The molar extinction coefficient of probe 1.

The absorbance values of probe 1 solutions at various concentrations (in PBS buffer, 10 mM, pH = 7.4) were measured at 332 nm. Each concentration was measured in triplicate, and the average value was taken. A standard curve was plotted with concentration (μM) as the abscissa and absorbance (A) as the ordinate, and linear fitting was performed according to the Beer-Lambert law:

$$A = \varepsilon\, b\, c$$

where:

A: absorbance; *b*: path length (1 cm); *c*: concentration.

4. Spectral analysis of probe with biothiol

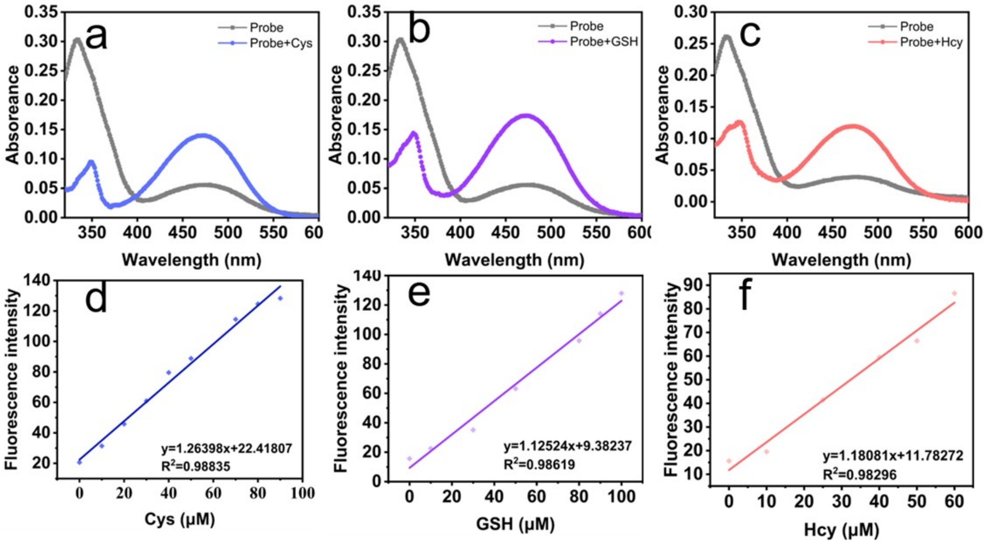

Fig. S7 (a-c): UV absorption spectra of probe 1 (10 μM） in PBS buffer (10 mM, pH=7.4). (d-f): Linear relationship between fluorescence intensity and biothiol.

5. The absorbance of the fluorophore compound 2 reacted with biothiols

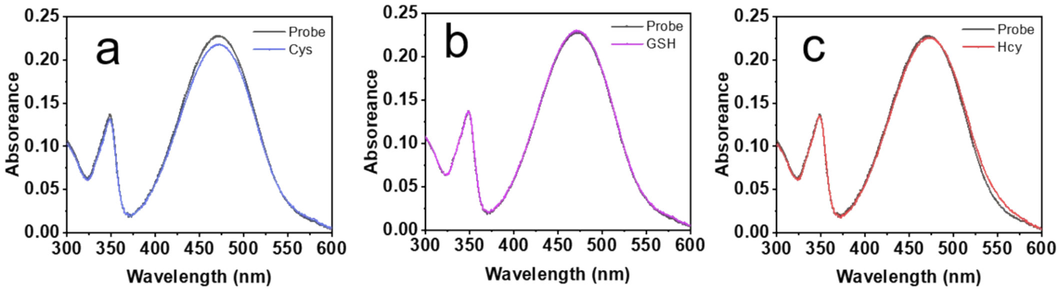

Fig. S8 (a-b): UV absorption spectra of fluorophore compound 2 (10 μM) reacted with biothiols in PBS buffer (10 mM, pH=7.4).

6. Fluorescence quantum yield

Using rhodamine B (RhB) as the standard reference, the absorbance and integrated fluorescence area of RhB, probe before and after reaction with GSH, were measured (ex: 475 nm; slit width: 10 nm). The fluorescence quantum yield of probe before the reaction (Φ_1) and after the reaction with GSH (Φ_2) were calculated according to the following formula[1-2]:

$$\Phi_{\text{sample}} = \Phi_{\text{std}} \times \frac{A_{\text{std}}}{A_{\text{sample}}} \times \frac{F_{\text{sample}}}{F_{\text{std}}} \times \left(\frac{n_{\text{sample}}}{n_{\text{std}}}\right)^2$$

where：

Φ_{std}： fluorescence quantum yield of RhB；
A： absorbance；
F：integrated area of the fluorescence emission spectrum；
n： refractive index of the solvent.

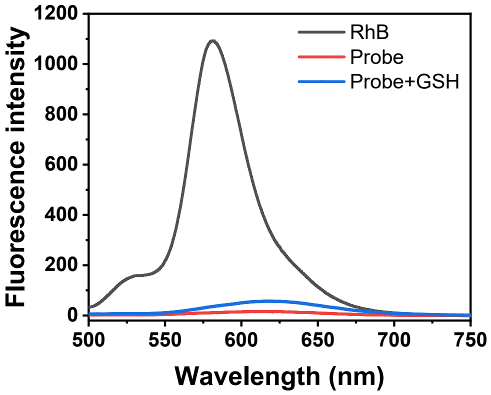

Fig.S9 The fluorescence spectra of RhB and Probe before/after the reaction

The fluorescence spectra of RhB and probe before and after the reaction are shown in Fig.S9. The absorbance values of RhB, probe before reaction, and probe after reaction were determined to be 0.027, 0.040, and 0.031, respectively. Substituting these values into the formula yielded a fluorescence quantum yield of $\Phi_1 = 0.011$ for Probe 1 before reaction and $\Phi_2 = 0.054$ for probe after reaction with GSH.

7. Kinetic Studies

The reaction rate constant of the probe with Cys, GSH, and Hcy was evaluated under pseudo-first-order kinetics conditions (10 μM probe and 100 μM biothiols). The reaction of probe with biothiols in aqueous conditions (PBS, 10 mM, pH=7.4) was monitored using the fluorescence intensity at 625 nm. The pseudo-first-order rate constant was determined by fitting the fluorescence intensities of the probe to the pseudo-first-order equation[3]:

$$\ln [(Fmax-Ft) / Fmax] = -k't$$

Where F_t and F_{max} are the fluorescence intensities at 625 nm at time t and the maximum value obtained after the reaction was completed. k′ is the pseudo-first-order rate constant. Figure S10-S12 are the pseudo-first-order plot for the reaction of probe with Cys, GSH, and Hcy, respectively. The negative slope of the line provides pseudo-first-order rate constant: *k′*.

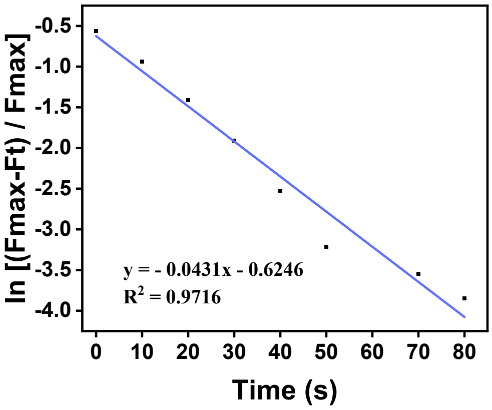

Fig. S10 Peudo-first-order kinetic plot of the reaction of probe incubated with Cys in aqueous conditions (PBS, 10 mM, pH=7.4). Slope = -0.0431 S^{-1}.

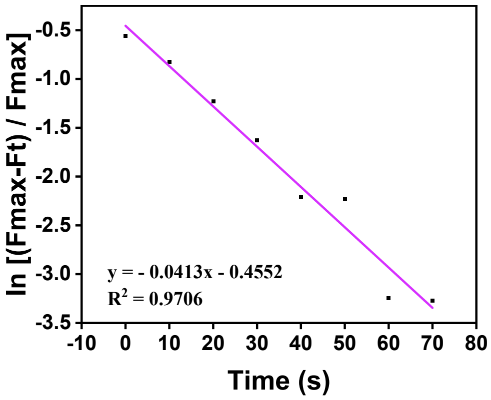

Fig.S11 Peudo-first-order kinetic plot of the reaction of probe incubated with GSH in aqueous conditions (PBS, 10 mM, pH=7.4). Slope = -0.0413 S^{-1}.

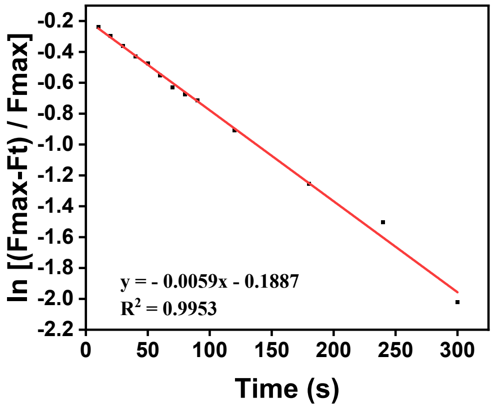

Fig.S12 Peudo-first-order kinetic plot of the reaction of probe incubated with Hcy in aqueous conditions (PBS, 10 mM, pH=7.4). Slope = -0.0059 S^{-1}.

Table S1 The pseudo-first-order rate constants for the reaction of probe 1 with Cys, GSH and Hcy

Biothiol	Cys	GSH	Hcy
K′	0.0431 S^{-1}	0.0413 S^{-1}	0.0059 S^{-1}

8. Reaction mechanism studies.

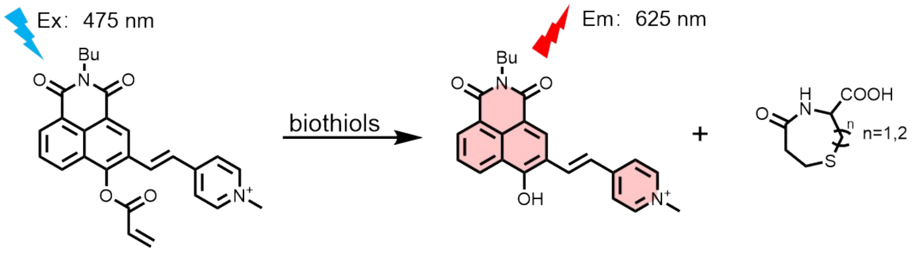

Probe 1

Scheme S2. The proposed response mechanism

The reaction mechanism of the probe reacting with Cys (5 equiv) in a solution (CH_3OD). After incubation of the mixture at room temperature for 30 min, the ^1H NMR in the reaction solution was measured. ^1H NMR displayed that the resonance signal from 6.3 to 6.9 ppm, corresponding to the double-bond of acrylate group, disappeared. The structure was further characterized by MS. Therefore, we confirmed that the reaction is based on our proposed reaction mechanism.

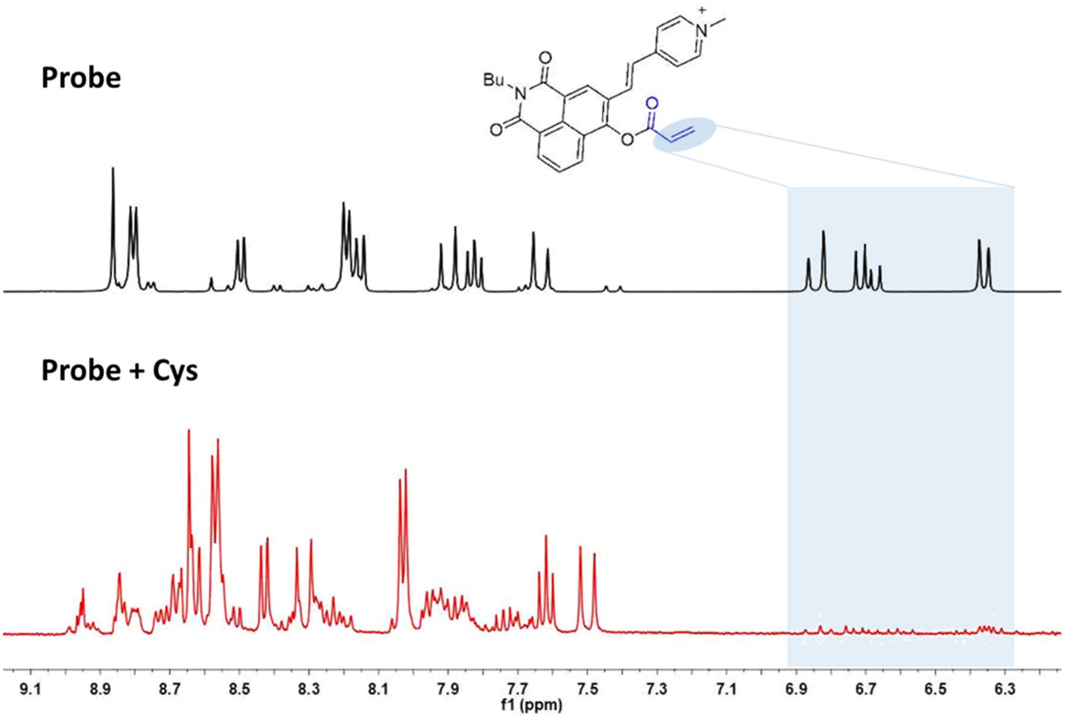

Fig. S13 ^1H NMR of the probe 1 with Cys dissolved in CH_3OD

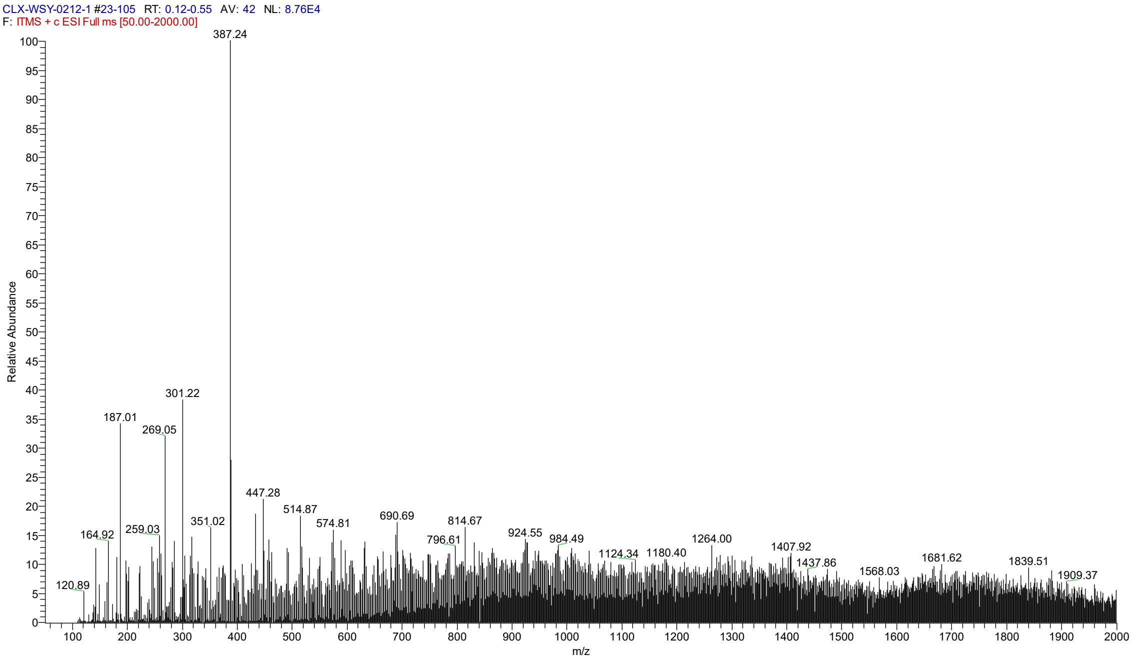

Fig. S14 The mass septrum of the probe reacted with Cys in PBS soultion (10 mM, pH=7.40)

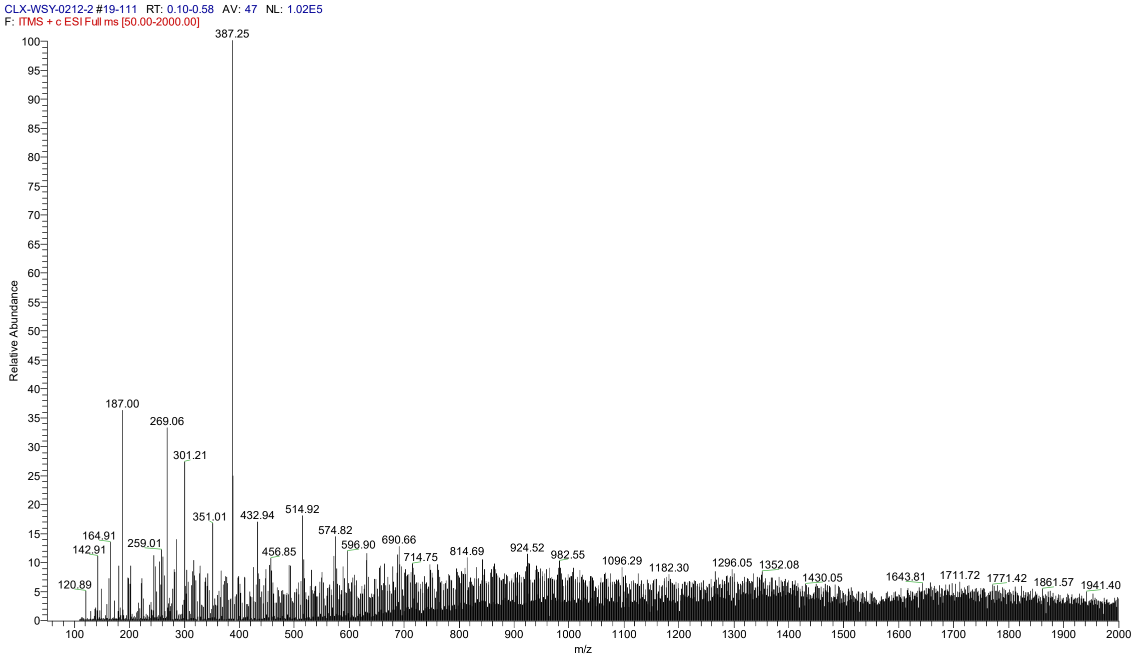

Fig. S15 The mass septrum of the probe reacted with Hcy in PBS soultion (10 mM, pH=7.40)

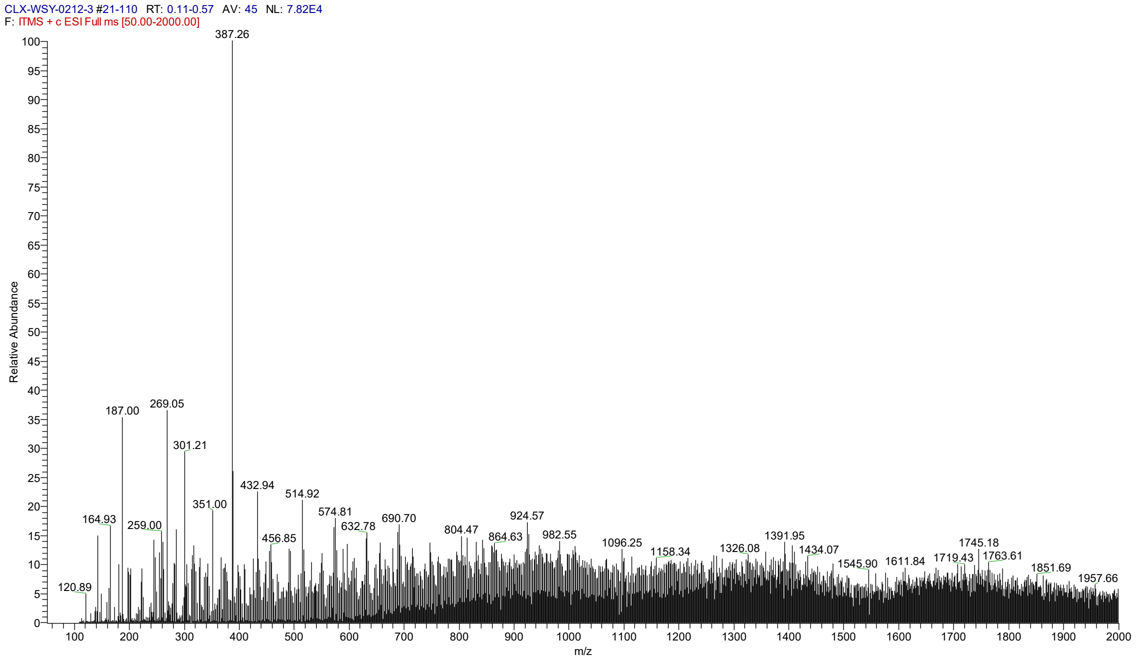

Fig. S16 The mass septrum of the probe reacted with GSH in PBS soultion (10 mM, pH=7.40)

9. Photostability of the probe 1

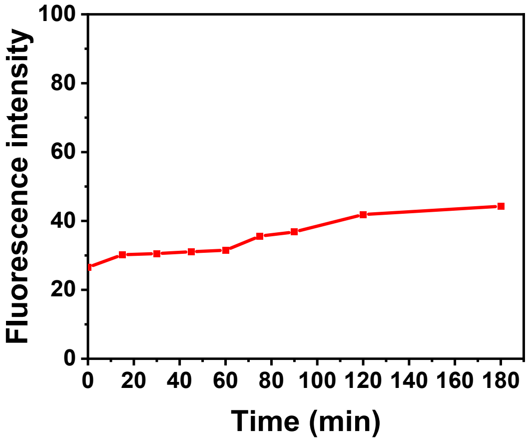

Fig. S17 The photostability of the probe.

10. pH stability of the probe

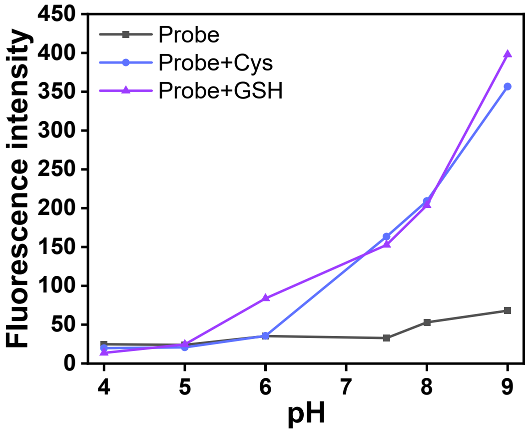

Fig. S18 Fluorescence spectra of probe 1 (10 µM) and probe 1 + biothiols (100 µM) as a function of pH (4.0–9.0).

11. CCK-8 assay

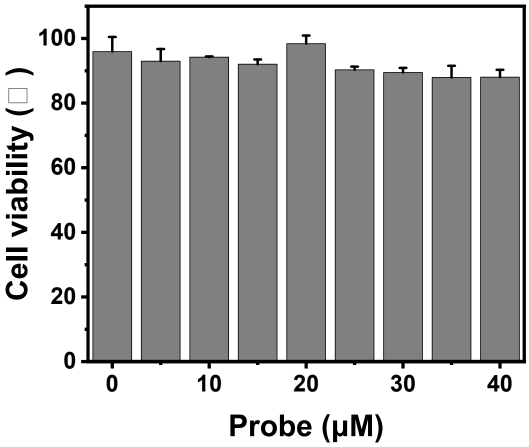

Fig. S19 The viability of HeLa cells after incubation with different concentrations of probe 1 (0-40 µM).

12. Preparation and Characterization of PMMA-Hg^{2+} Complexes

To study adsorption kinetics, 100 mg PMMA-NPs were mixed with 60mL 5µM Hg^{2+} solution. A 60 ml mixture was stirred at a temperature of 290 K, with a speed of 180 rpm, and sampling was conducted at various time intervals up to 12 hours. After centrifuging the sample (8000 r/min, 5 min), the supernatant was filtered using a 0.22 µm membrane, and the Hg^{2+} concentration in the solution was determined by ICP-MS. The precipitate was dried (323 K, 300 min) for SEM characterization.

The particle size and zeta potential of PMMA and PMMA-Hg^{2+} were measured using a Malvern Zetasizer Nano ZS90. First, the PMMA suspension was diluted with deionized water until clear, and 1.5 mL of the solution was taken for particle size and zeta potential measurements. For the PMMA-Hg^{2+} sample, the pre-adsorbed PMMA particles were mixed with deionized water and treated by ultrasonication for 20 min to prepare the PMMA-Hg^{2+} suspension. The suspension was then diluted with deionized water to a clear state for particle size and zeta potential measurement. The experiment was repeated three times, and the results were averaged.

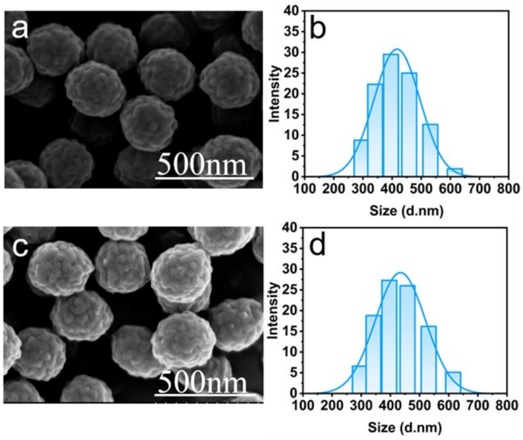

Fig.S20 Morphological Characterization. (a-b): SEM and size of PMMA, (c-d): SEM and size of PMMA-Hg^{2+} complexes.

13. Imaging of endogenous biothiol and ROS levels in HeLa cells under PMMA or PMMA-Hg^{2+} complexes exposure for 4h

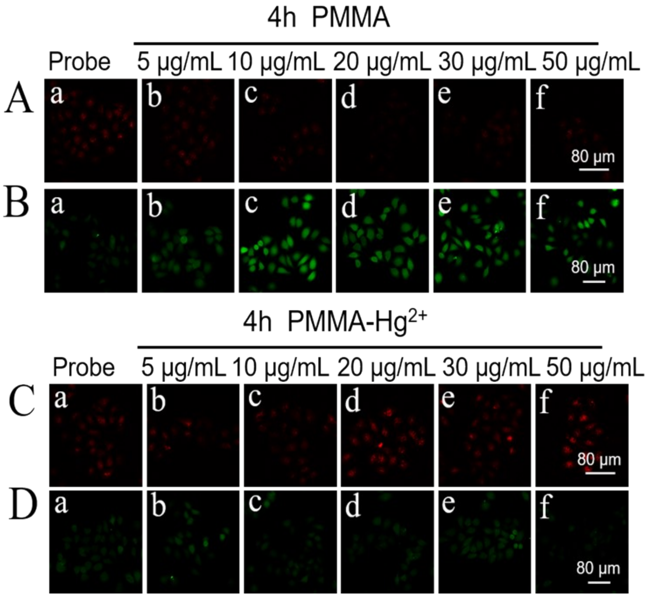

Fig. S21 (A) and (B): Imaging of endogenous biothiol and ROS levels in HeLa cells under PMMA exposure (4 h). (C) and (D): Imaging of endogenous biothiol and ROS levels in HeLa cells under PMMA-Hg^{2+} co-exposure (4 h).

14. CQ Pre-experiment

According to a literature search, we found that the effective concentration of CQ for lysosomal inhibition in cells ranges from 10 to 100 μM[4-7]. Moreover, it has been reported that the IC_{50} of CQ against HepG2 cells falls within the range of 25-50 μM. Therefore, we initially treated cells with 50 μM CQ for 24 hours; however, this resulted in extensive cell death. We then treated cells with 20 μM CQ for 24 hours. Under this condition, a remarkable increase in intracellular fluorescence intensity was observed across all cells, including the control group. Considering that CQ itself may be a source of oxidative stress, we decided to keep the CQ concentration unchanged (20 μM) but shorten the treatment duration to 6 h for subsequent experiments to avoid confounding effects on the results.

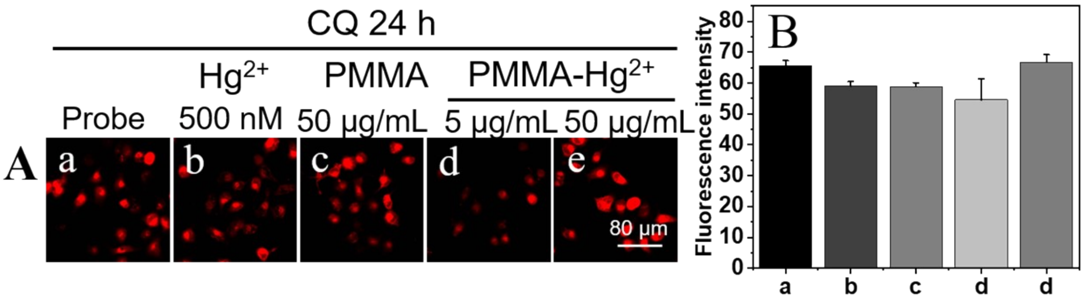

Fig. S22 (A): Imaging of endogenous biothiol levels in HeLa cells under Single or combined PMMA/Hg^{2+} exposure (30 min) (A): HeLa cells respectively pretreated with CQ (20 μM, 24 h) before imaging of endogenous biothiol levels under Single or combined PMMA/Hg^{2+} exposure (30 min). (B): Relative mean fluorescence intensities (n=3; SD) of (A).

References:

1. A. M. Brouwer, Pure and Applied Chemistry, 2011, **83**, 2213-2228.
2. C. Würth, M. Grabolle, J. Pauli, M. Spieles and U. Resch-Genger, Nature Protocols, 2013, **8**, 1535-1550.
3. J. Sun, L. Zhang, X. Zhang, Y. Hu, C. Ge and J. Fang, Analyst, 2016, **141**, 2009-2015.
4. E. S. Prokopenko, T. V. Sokolova, O. V. Nadei, A. D. Trubnikova and N. I. Agalakova, Journal of Evolutionary Biochemistry and Physiology, 2024, **60**, S135-S147.
5. T. le van, H.-T. Phan-Thi, M.-X. Huynh-Thi, T. Dang Minh, A. Holterman, G. Grassi, U. Nguyễn Lưu Thảo and T. Nhung, Cells, 2023, **12**, 1025.
6. J.-S. Syu, T. Baba, J.-Y. Huang, H. Ogawa, C.-H. Hsieh, J.-X. Hu, T.-Y. Chen, T.-C. Lin, M. Tsuchiya, K.-I. Morohashi, B.-M. Huang, F.-l. Lu and C.-Y. Wang, Scientific Reports, 2017, **7**, 240.
7. S.-H. Su, S.-J. Su, L.-Y. Huang and Y.-C. Chiang, Free Radical Biology and Medicine, 2023, **198**, 1-11.